

Heptazine, Cyclazine, and Related Compounds: Chemically-Accurate Estimates of the Inverted Singlet–Triplet Gap

Pierre-François Loos, Filippo Lipparini, and Denis Jacquemin*



Cite This: *J. Phys. Chem. Lett.* 2023, 14, 11069–11075



Read Online

ACCESS |



Metrics & More

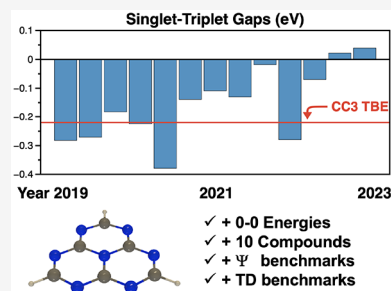


Article Recommendations



Supporting Information

ABSTRACT: Molecules that violate Hund's rule and exhibit an inverted gap between the lowest singlet S_1 and triplet T_1 excited states have attracted considerable attention due to their potential applications in optoelectronics. Among these molecules, the triangular-shaped heptazine, and its derivatives, have been in the limelight. However, conflicting reports have arisen regarding the relative energies of S_1 and T_1 . Here, we employ highly accurate levels of theory, such as CC3, to not only resolve the debate concerning the sign but also quantify the magnitude of the S_1 – T_1 gap. We also determined the 0–0 energies to evaluate the significance of the vertical approximation. In addition, we compute reference S_1 – T_1 gaps for a series of 10 related molecules. This enables us to benchmark lower-order methods for future applications in larger systems within the same family of compounds. This contribution can serve as a foundation for the design of triangular-shaped molecules with enhanced photophysical properties.



In many technological applications that rely on either light-energy or energy-light conversions, it is essential to control the energy gap that separates the relevant electronic excited states (ESs). Specifically, the magnitude of the singlet–triplet gap (STG), the energy difference between the lowest-energy singlet excited state, S_1 , and the lowest-energy triplet state, T_1 , is of prime importance, as key photophysical events typically take place in these states. For example, to design highly fluorescent molecules, a large STG is sought to minimize the $S_1 \rightarrow T_1$ intersystem crossing. In contrast, in the pursuit of efficient third-generation organic light-emitting diodes (OLEDs), a vanishingly small STG is required to maximize the reverse intersystem crossing ($T_1 \rightarrow S_1$), resulting in the production of more photons.

Despite constant developments, experimental characterizations of ESs remain costly and challenging. This is why theoretical models, which explore the ES nature and energies, are frequently employed hand-in-hand with experimental measurements. Nevertheless, theoretical methods also face challenges in achieving chemically accurate (i.e., error of the order of ± 0.05 eV) estimates of ES energies for nontrivial molecular systems. This is in stark contrast with ground-state (GS) properties, for which a panel of reliable black-box methods is now readily available. The search for molecular structures having specific, original, and tunable ES properties are therefore extremely active research lines.

In 2019, two groups independently published seminal works showing that some triangulenes do not adhere to Hund's rule, with T_1 being found above S_1 .^{1,2} On the one hand, Ehrmaier and co-workers demonstrated that this inversion takes place in heptazine (compound 1 in Figure 1),¹ whereas, on the other hand, de Silva reported negative STG in cyclazine (compound

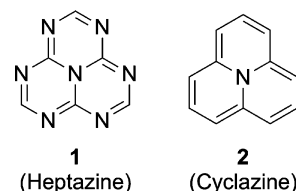


Figure 1. Representation of heptazine and cyclazine.

2 in Figure 1).² These remarkable and unexpected discoveries, supported by both theoretical and experimental analyses (as discussed below),^{1,2} stimulated many subsequent works.^{3–13} In particular, several groups analyzed in detail the reasons behind this deviation from Hund's rule,^{3,8,11,12,14} and concurrently, improved substituted molecules have been designed using various modeling approaches.^{4,8,15,16}

In the original work of Ehrmaier et al., a series of wave function calculations performed with the double- ζ cc-pVDZ basis set was used to estimate the STG of heptazine (see Table 1). This investigation revealed that time-dependent density-functional theory (TD-DFT) relying on global hybrids—the typical workhorse for ES calculations—failed to deliver qualitatively correct values.¹ Notably, the most sophisticated levels of theory used in ref 1, namely, coupled-cluster with

Received: October 30, 2023

Revised: November 22, 2023

Accepted: December 1, 2023

Published: December 4, 2023

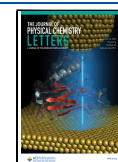


Table 1. Vertical Transition Energies to the Lowest S_1 and T_1 ESs, as Well as the Corresponding STG of Heptazine Obtained with Various Levels of Theory (All Values in eV)^a

Method	S_1	T_1	STG	ref	Year
ADC(2)/cc-pVDZ	2.569	2.851	-0.282	1	2019
CC2/cc-pVDZ	2.676	2.947	-0.271	1	2019
CCSD/cc-pVDZ	2.791	2.963	-0.182	1	2019
CASPT2/cc-pVDZ	2.326	2.551	-0.225	1	2019
SCS-CC2/def2-TZVP	2.847	3.226	-0.379	3	2021
SC-NEVPT2/def2-TZVP	3.259	3.398	-0.139	3	2021
ADC(3)/cc-pVDZ	2.665	2.774	-0.109	4	2021
RASPT2/def2-TZVP	2.54	2.67	-0.13	6	2022
XMC-QDPT2/def2-TZVP			-0.018	9	2022
Mk-MRCCSD(T)/def2-TZVP			-0.28	11	2023
ADC(3)/cc-pVTZ	2.81	2.88	-0.07	13	2023
Δ CCSD(T)/aug-cc-pVDZ			+0.022	13	2023
Δ CCSD(T)/cc-pVTZ			+0.039	13	2023
ADC(2)/aug-cc-pVTZ	2.675	2.921	-0.246	This work	
CC2/aug-cc-pVTZ	2.767	3.006	-0.239	This work	
CCSD/aug-cc-pVTZ	2.953	3.087	-0.134	This work	
CC3/aug-cc-pVDZ	2.693	2.898	-0.205	This work	
TBE ^b	2.717	2.936	-0.219	This work	

^aThe present calculations are performed on the CCSD(T)/cc-pVTZ GS structure. Note that previous works used (slightly) different geometries.

^bTheoretical best estimate obtained from CC3/aug-cc-pVTZ + [CCSDT/6-31+G(d) - CC3/6-31+G(d)] for S_1 and CC3/aug-cc-pVDZ + [CCSD/aug-cc-pVTZ - CCSD/aug-cc-pVDZ] for T_1 .

singles and doubles (CCSD) and the complete-active-space self-consistent-field method with second-order perturbative correction (CASPT2), provided smaller STG than less advanced second-order approaches (Table 1).

Two years later, Ricci et al. relied on a significantly larger basis set, def2-TZVP, and reported a STG of -0.139 eV at the N -electron valence state second-order perturbation theory (NEVPT2) level using a large (12,12) active space.³ The STG value of Ghosh and Bhattacharyya computed with the restricted-active-space method (RASPT2) is similar to the NEVPT2 value (-0.13 eV), whereas similarity-transformed equation-of-motion CCSD (STEOM-CCSD) unexpectedly yields a much larger result (-0.66 eV).⁶ A comparison between the multireference values of ref 1,3, and 9 also hints that increasing the size of the basis set from cc-pVDZ to def2-TZVP induces a significant drop of the STG magnitude. In 2022, new experiments were carried out for two substituted heptazines, and a tiny yet negative gap (-0.011 eV) was found for one of them,⁷ whereas very recently, Actis et al. reported a negative STG of approximately -0.2 eV in an extended carbon-nitride (CN) graphite-like structure.¹⁷

Very recently, Dreuw and Hoffmann went a step further by questioning the existence of an inverted STG in heptazine and two closely related molecules (cyclazine, **2**, and cycloborane).¹³ By systematically ramping up the degree of the algebraic-diagrammatic construction (ADC), going from ADC(2)-s, to ADC(2)-x, and then ADC(3), they observed clear reductions of the STGs, with an ADC(3)/cc-pVTZ gap amounting to a mere -0.07 eV. In addition, they conducted (state-specific) Δ CC calculations based on non-Aufbau reference determinants with a series of increasingly larger basis sets and obtained a positive STG of +0.04 eV with their most refined approach, namely, Δ CCSD(T)/cc-pVTZ. In short, as the level of theory became more accurate, the negative character of the STG in heptazine diminished. Dreuw and Hoffmann, therefore, concluded that the sign (amplitude) of the STG of heptazine was uncertain (notably small),

emphasizing the necessity for more accurate calculations¹³ This Letter answers their call.

To obtain very accurate estimates of the ES energies of heptazine, i.e., theoretical best estimates (TBEs), we employed CC methodologies including singles, doubles, and iterative triples, along with large basis sets (see computational details section). This approach represents a substantial advancement in comparison with earlier studies. First, we optimized the D_{3h} GS structure of heptazine at the CCSD(T)/cc-pVTZ level, ensuring a solid starting point for further calculations. Next, we performed a series of equation-of-motion CC (EOM-CC) calculations with various diffuse-containing basis sets, up to third-order CC (CC3) for the triplet state, and even using full triples (CCSDT) for the singlet state (see the Supporting Information for the complete set of data). Importantly, we did not consider state-specific approaches such as Δ SCF and Δ CC, but systematically relied on linear response theory to directly target ES energies. In a previous benchmark devoted to the ESs of bicyclic derivatives, CC3 was found significantly more accurate than CC schemes relying on perturbative triples.¹⁸

It is important to note that the so-called (GS) T_1 -diagnostic¹⁹ returns a value of 0.02 at the CCSD/aug-cc-pVTZ level for heptazine, indicating the absence of significant multireference character in the GS. Furthermore, our CC3/aug-cc-pVDZ reveals no substantial double excitation character with % T_1 values (which indicates the percentage of single excitation character) of 86.3% and 95.7% for the lowest excited singlet and triplet states, respectively. These observations are consistent with both previous conclusions drawn at the second-order CC level,⁹ and the negligible difference observed between CC3 and CCSDT for the S_1 excitation energy (<0.01 eV, see the Supporting Information). There is therefore no clear reason to delve into multiconfigurational methodologies here, as the CC family of systematically improvable methods appears to offer the most efficient path to chemical accuracy.

Table 2. Vertical Transition Energies to the lowest S_1 and T_1 ESs, as Well as Corresponding STG of Cyclazine Obtained with Various Levels of Theory (All Values in eV)^a

Method	S_1	T_1	STG	ref	Year
CIS(D)/cc-pVDZ	1.07	1.37	-0.30	2	2019
ADC(2)/cc-pVDZ	1.04	1.20	-0.16	2	2019
CCSD/cc-pVDZ	1.09	1.19	-0.10	2	2019
SCS-CC2/def2-TZVP	1.110	1.334	-0.224	3	2021
SC-NEVPT2/def2-TZVP	1.224	1.288	-0.044	3	2021
ADC(3)/cc-pVDZ	0.777	0.869	-0.092	4	2021
RASPT2/def2-TZVP	0.86	0.89	-0.03	6	2022
XMC-QDPT2/def2-TZVP			-0.106	9	2022
CC3/cc-pVDZ	0.98	1.15	-0.17	10	2023
Mk-MRCCSD(T)/def2-TZVP			-0.18	11	2023
ADC(3)/cc-pVTZ	0.81	0.87	-0.06	13	2023
Δ CCSD(T)/aug-cc-pVDZ			+0.015	13	2023
Δ CCSD(T)/cc-pVTZ			+0.025	13	2023
ADC(2)/aug-cc-pVTZ	1.001	1.138	-0.137	This work	
CC2/aug-cc-pVTZ	1.051	1.181	-0.130	This work	
CCSD/aug-cc-pVTZ	1.090	1.154	-0.064	This work	
CC3/aug-cc-pVDZ	0.990	1.121	-0.131	This work	
TBE ^b	0.979	1.110	-0.131	This work	

^aThe present calculations are performed on the CCSD(T)/cc-pVTZ GS structure. Note that previous works used (slightly) different geometries. The experimental absorption of cyclazine in hexane was measured at 0.972 eV.²¹ ^bTheoretical best estimate obtained from CC3/aug-cc-pVTZ + [CCSDT/6-31+G(d) - CC3/6-31+G(d)] for S_1 and CC3/aug-cc-pVDZ + [CCSD/aug-cc-pVTZ - CCSD/aug-cc-pVDZ] for T_1 .

In the extended QUEST database,²⁰ it was found that the typical error associated with CC3 is as small as 0.02 eV for such well-behaved ESs (having % $T_1 > 85\%$). We are therefore reasonably confident that the data reported in Table 1 stand as the most reliable to date and are likely chemically accurate (errors below 0.05 eV). As reported in Table 1, our TBE values for the singlet and triplet states are respectively 2.717 and 2.936 eV, resulting in a negative gap of -0.219 eV. It is no surprise that this value is in between the CC2 and CCSD results obtained with large basis sets. Second-order methods such as ADC(2) and CC2 tend to overestimate the magnitude of the STG, while CCSD and ADC(3) exhibit a tendency to provide an error in the opposite direction. We note that in the QUEST database,²⁰ CCSD was found to overshoot the triplet (singlet) energies by 0.03 (0.14) eV on average, whereas ADC(3) was found to underestimate triplet (singlet) excitation energies by -0.18 (-0.08) eV, which is consistent with the present trends. We also note that previous CASPT2 (NEVPT2) significantly underestimates (overestimates) the absolute energies of S_1 and T_1 . Finally, it appears that the aug-cc-pVDZ basis set proves sufficiently large to deliver accurate results (at the CC3 level) while the cc-pVDZ basis set produces an excessively negative STG. In any case, the data showcased in Table 1 conclusively affirm that the vertical excitation energy of T_1 in heptazine is approximately 0.22 eV higher than that of S_1 .

In Table 2, we provide a similar comparative analysis, juxtaposing our present estimates with prior data from the literature for the singlet and triplet vertical excitation energies of cyclazine (compound 2 in Figure 1). While the two states are notably closer to the GS than in heptazine, the methodological trends outlined in the previous paragraph for heptazine mostly pertain. For example, using a small basis set yields STGs that are too negative, whereas CCSD and ADC(3) underestimate the gap. For cyclazine, both ADC(2) and CC2 overestimate the excitation energies, but they provide an excellent estimate of the STG, with SCS-CC2 being

significantly off. Our TBE for the STG in cyclazine is -0.131 eV, which is large enough to affirm the gap inversion in this system.

Let us now turn toward the 0-0 energies of heptazine, as this property provides a reliable basis for comparisons with experimental data.²² For obvious computational reasons, we use CCSD/cc-pVDZ, as well as its EOM-CCSD and unrestricted variants (UCCSD) to determine the geometries and vibrational frequencies of S_0 , S_1 , and T_1 , respectively. While the geometries obtained are not as accurate as those computed at the CCSD(T)/cc-pVTZ level (see above and below), it should be stressed that the 0-0 energies are known to be less sensitive to the accuracy of the employed structures than vertical excitation energies.²³ Besides, the CC3/aug-cc-pVDZ vertical S_1 excitation energy computed on the CCSD/cc-pVDZ geometry is 2.649 eV, which is quite close to the 2.693 eV result obtained with the CCSD(T)/cc-pVTZ structure. Nevertheless, the use of different levels of theory for the singlet and triplet geometries likely results in a 0-0 STG value significantly less accurate than that of its vertical counterpart.

Starting from the planar D_{3h} GS geometry, the EOM-CCSD optimization of S_1 led to one imaginary frequency associated with puckering of the central nitrogen atom. The true minimum of the S_1 structure presents a C_{3v} point group symmetry (see Figure 2). The CC3/aug-cc-pVTZ S_0 - S_1

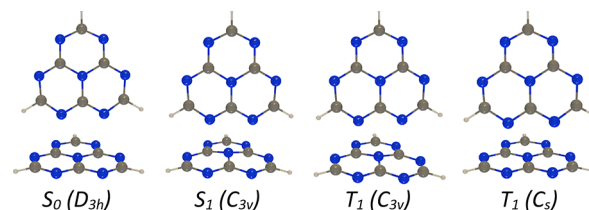


Figure 2. Two different views of the CCSD, EOM-CCSD, and UCCSD optimized geometries obtained with the cc-pVDZ basis set.

adiabatic energy, E^{adia} , is 2.550 eV, which can be corrected by the difference of zero-point vibrational energies between both states ($\Delta E^{\text{ZPVE}} = -0.044$ eV) determined at the (EOM-)CCSD/cc-pVDZ level to obtain a 0–0 TBE of 2.506 eV for the S_0 – S_1 transition. The difference of approximately -0.2 eV between the 0–0 and vertical transition energies aligns with the typical corrections observed for relatively rigid molecules.^{24–26} On a methodological note, at the CCSD(T)(a)*/*aug-cc-pVTZ* level, we get $E^{\text{adia}} = 2.671$ eV ($E^{0-0} = 2.627$ eV), for the S_0 – S_1 transition, a value 0.12 eV larger than the CC3 result. This data is likely more directly comparable to the results obtained for the triplet state below, for which CCSD with perturbative triples is used to obtain the TBE.

For the lowest triplet, the D_{3h} optimal structure shows two imaginary frequencies at the UCCSD/cc-pVDZ level. The first one leads to a puckered C_{3v} geometry similar to the S_1 case, and the second one corresponds to an in-plane deformation providing a C_s geometry, the C_{3h} structure being unstable (Figure 2). Both the C_{3v} and C_s structures are genuine minima and have quite similar energies. For the former, the UCCSD(T)/*aug-cc-pVTZ* value for E^{adia} is 3.154 eV and the CCSD-based ZPVE correction is quite large (-0.189 eV) leading to a 0–0 transition at 2.965 eV. For the latter, we get $E^{\text{adia}} = 3.038$ eV and $E^{0-0} = 3.057$ eV, this structure showing an uncommon positive ZPVE correction. In any case, the 0–0 energies of these two triplet structures are clearly larger than the 2.627 eV estimate obtained with a comparable level of theory for S_1 . In other words, the negative STG obtained from the vertical transitions (-0.219 eV) does not change sign when considering geometry relaxation and zero-point vibrational effects. It apparently seems to become slightly larger (-0.338 eV), although we acknowledge that the latter value is not chemically accurate due to the increased number of approximations made. Nevertheless, previous works also observed that the inverted STG found through vertical calculations persists when considering 0–0 energies.^{1,4,27}

Of course, the state-of-the-art methods discussed above are not readily applicable to the design of novel compounds with enhanced properties, a goal typically achieved through the addition of side substituents or the extension of the conjugated core.^{4,8,15,16,27,28} A wide panel of strategies has been explored in the literature to design new compounds, but the challenge lies in the absence of definitive benchmark values. This lack of a clear reference is evident, for instance, in the varying choices of reference methods made by different research groups when benchmarking double-hybrid functionals, with some using SCS-CC2²⁹ and others opting for CCSD.^{30,31}

Hence, we decided to perform a benchmark of lower-order approaches for a set of 10 triangulenes, including heptazine, cyclazine, and eight additional molecules displayed in Figure 3, for which we obtained accurate TBE/*aug-cc-pVTZ* values using the same procedure as that in Tables 1 and 2. The selection of these molecules was inspired by previous literature.^{9,11,29} We underline that the magnitude of the STG varies significantly within this series, as do the absolute singlet and triplet excitation energies (see Table S1 in Supporting Information). The TBEs for the STG, listed in Table 3, range from -0.029 eV (8) to -0.305 eV (10) and thus cover a significant range of possibilities. With these TBE values in hand, we conducted an evaluation of the performance of second-order wave function methods, specifically CIS(D), ADC(2), CC2, and some of their spin-scaled variants (SOS-ADC(2), SCS-ADC(2), SOS-CC2 and SCS-CC2), as well as

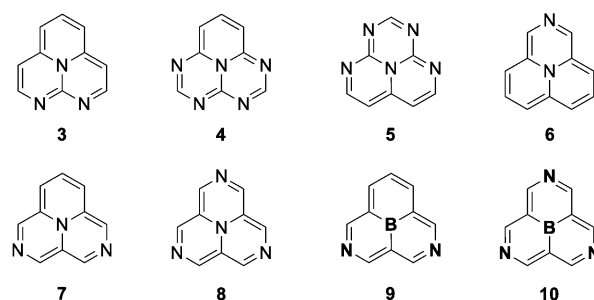


Figure 3. Representation of the eight additional molecules considered in the present benchmark set.

Table 3. Theoretical Best Estimates Obtained for All Compounds Considered Here (All Values in eV)^a

Compound	S_1	T_1	STG
1	2.717	2.936	-0.219
2	0.979	1.110	-0.131
3	1.562	1.663	-0.101
4	2.177	2.296	-0.119
5	2.127	2.230	-0.103
6	0.833	0.904	-0.071
7	0.693	0.735	-0.042
8	0.554	0.583	-0.029
9	1.264	1.463	-0.199
10	1.522	1.827	-0.305

^aSee Table S1 in the Supporting Information for details and raw data.

CCSD. We also benchmarked double hybrid functionals within the TD-DFT framework. More specifically, we tested four of them, namely PBE0-2, SOS-PBE-QIDH, SCS-PBE-QIDH, and SOS-RSX-QIDH, as these were previously identified as promising candidates for this particular task in a benchmark study performed by Sancho-Garcia, Adamo, and co-workers.²⁹ All results can be found in Tables S2 and S3 of Supporting Information.

The results of this benchmark for the STG are displayed in Table 4 in which we report the mean signed error (MSE), the mean absolute error (MAE), and the standard deviation of the

Table 4. MSE, MAE, and SDE (in eV) Determined for the STG, Considering Our TBE of Table S1 as Reference

Method	MSE	MAE	SDE
CIS(D)	-0.253	0.253	0.083
ADC(2)	-0.033	0.033	0.035
SOS-ADC(2)	-0.193	0.193	0.089
SCS-ADC(2)	-0.115	0.115	0.019
CC2	-0.027	0.027	0.041
SOS-CC2	-0.165	0.165	0.031
SCS-CC2	-0.111	0.111	0.021
CCSD	+0.081	0.081	0.014
PBE0-2 ^a	-0.066	0.114	0.235
SOS-PBE-QIDH	-0.073	0.075	0.084
SCS-PBE-QIDH	-0.033	0.055	0.085
SOS-RSX-QIDH	-0.084	0.105	0.121

^aFor PBE0-2, 6 is a clear outlier due to a strong orbital mixing in the triplet state (see the Supporting Information). Removing it yields MSE, MAE, and SDE of 0.006, 0.046, and 0.056 eV, respectively. Note, however, that removing this challenging compound would improve the statistics of all other double-hybrid functionals.

errors (SDE) using our TBEs as reference. Equivalent statistical analyses for the singlet and triplet energies themselves can be found in Tables S4 and S5 of Supporting Information. Notably, all tested wave function approaches, except for CCSD, yield a negative MSE, indicating an overestimation of the magnitude of the (negative) STGs. This trend is particularly pronounced for CIS(D), and the four “spin-scaled” second-order approaches. In contrast, CCSD tends to provide smaller STG estimates, with no inversion observed for both 7 and 8, for which our TBEs are slightly negative. As one can see by comparing the MSEs and MAEs, these trends are systematic. All wave function approaches, except for CIS(D), provide acceptable SDEs, correctly predicting the chemical trends in the series, which is a satisfying outcome. Among these methods, the most refined scheme, CCSD, produces the smallest SDE, while, as expected,²⁰ the two spin-scaled CC2 models also provide more consistent values than the standard CC2 approach. In contrast, at the ADC(2) level, only the SCS approach improves the SDE.

Taking into consideration the usual trade-off between absolute and relative accuracies as well as the computational cost, ADC(2) stands out as the most suitable cost-effective option for assessing the STG in similar systems. It is also noteworthy that ADC(2) delivers satisfactory absolute singlet and triplet energies (see Tables S4 and S5 in the Supporting Information). Shifting our focus to the TD-DFT results, it is important to highlight that PBE0-2 fails to provide a reasonable triplet energy for the challenging compound 6, which very badly affects its otherwise satisfactory statistics. All three QIDH-derived functionals tend to magnify the negative character of the STG and yield relatively large SDEs, equal to or larger than those of CIS(D). Among the double-hybrid functionals tested, SCS-PBE-QIDH proves to be the most reliable, though it offers less consistent results than ADC(2).

Finally, we also consider cycloborane, the equivalent of cyclazine 2 but with a central boron atom instead of a nitrogen atom. This compound has been previously studied by Dreu and Hoffmann.¹³ As detailed in Section S3 of the Supporting Information, the D_{3h} structure presents an inverted STG. Yet this GS geometry is not a genuine minimum (one imaginary frequency at the MP2 level) and there exists a C_{3h} GS structure, approximately 1 kcal·mol⁻¹ more stable than the D_{3h} conformer at the CCSD(T)/cc-pVTZ level. This C_{3h} structure exhibits a clear bond length alternation and conforms to Hund's rule (Table S6). Consequently, this structure was not included in the benchmark discussed above.

In short, this contribution conclusively demonstrates that compounds 1–6, 9, and 10 indeed exhibit inverted vertical STGs. While 7 and 8 also deviate from Hund's rule according to our TBEs, the amplitudes of their negative STG are likely too small to be definitive. For both the lowest triplet and singlet states of all of these compounds, we performed CC3/CCSDT calculations with various diffuse-containing basis sets, as no indications of multireference character or a double-excitation nature were detected. For heptazine, neither the relaxation of the geometry in the excited states nor the inclusion of vibrational corrections alters the conclusion reached in the vertical approximation. In other words, the inverted STG persists when considering 0–0 energies.

When assessing the performance of lower-order methods suitable for computing the properties of substituted or extended triangulenes using our TBE values, we found that

ADC(2) likely strikes the best balance between accuracy, consistency, and cost among the wave function methods. While less consistent than ADC(2), the SCS-PBE-QIDH double-hybrid functional shows promise for TD-DFT calculations. We hope that this Letter can serve as the starting point for the accurate design of systems displaying inverted STGs.

COMPUTATIONAL DETAILS

General Information. All calculations rely on the frozen-core (FC) approximation and, except when noted, the default convergence thresholds and algorithms of a given code. In the text, we dropped the EOM/LR prefix for the CC methods, since the two formalisms provide the same transition energies.

Geometries. All GS structures were first optimized at the MP2/6-311G(d,p) level with GAUSSIAN 16.A.03,³² using a Z-matrix enforcing the highest possible point group symmetry. Tight convergence thresholds were applied during these optimizations. Analytical frequency calculations were next performed at the same level of theory, confirming that the structures are true minima. These stable MP2(FC)/6-311G(d,p) geometries were considered as starting point for CCSD(T)/cc-pVTZ analytical optimizations that were performed with CFOUR.^{33,34}

For the 0–0 calculations on heptazine, the GS geometry was reoptimized at the CCSD/cc-pVDZ level of theory, and vibrational frequencies were determined as well at this level using GAUSSIAN.³² The structure and vibrational frequencies of the lowest triplet were obtained with the same code at the UCCSD/cc-pVDZ level, whereas we applied the corresponding EOM-CCSD/cc-pVDZ level for the lowest singlet ES. Symmetry was lowered when imaginary frequencies were obtained, and the process was restarted until a true minimum was reached.

Transition Energies. We used a variety of quantum chemistry software to determine vertical transition energies, using three Gaussian basis sets containing both polarization and diffuse functions, namely 6-31+G(d), *aug-cc-pVDZ*, and *aug-cc-pVTZ*. This allowed us to obtain TBEs, following the formulas given in the footnotes of Tables 1 and 2, which assume that basis set effects are transferable at the CC levels, an approximation that we have extensively assessed and validated in one previous work.³⁵ CCSD calculations have been performed with DALTON³⁶ and GAUSSIAN.³² CC3³⁷ calculations have been performed with DALTON³⁶ as well as CFOUR,^{33,34} the latter allowing calculations for singlet ES only. CCSDT³⁸ calculations were also carried out with CFOUR and were only possible with the most compact basis set. The same code was used for the CCSD(T)(a)*³⁹ and single-point UCCSD(T) calculations with the triple- ζ basis set. In CFOUR, we relied on the QC-SCF algorithm⁴⁰ with the correct occupation number set, and a SCF convergence threshold of 10⁻⁹ or 10⁻¹⁰ au. All CIS(D),⁴¹ ADC(2),⁴² and CC2⁴³ calculations have been performed with TURBOMOLE^{44,45} using the *aug-cc-pVTZ* basis set and applying the RI approach⁴⁶ with the corresponding auxiliary basis. In these calculations, we enforced the default TURBOMOLE scaling parameters for SOS-ADC(2), SCS-ADC(2), SOS-CC2 and SCS-CC2. The TD-DFT calculations based on double hybrids were all performed with ORCA,⁴⁷ selecting PBE0-2,⁴⁸ SOS-PBE-QIDH,⁴⁹ SCS-PBE-QIDH,⁴⁹ and SOS-RSX-QIDH⁴⁹ and also using the FC approach. In ORCA, we set the tightSCF and grid3 options, with the *aug-cc-pVTZ* and the automatically generated auxiliary basis sets.

Note that the Tamm–Dancoff approximation was not enforced in the TD-DFT calculations.

■ ASSOCIATED CONTENT

SI Supporting Information

The Supporting Information is available free of charge at <https://pubs.acs.org/doi/10.1021/acs.jpcllett.3c03042>.

Full benchmark results, molecular orbital plots, cyclo-borane results; Cartesian coordinates (PDF)

■ AUTHOR INFORMATION

Corresponding Author

Denis Jacquemin – Nantes Université, CNRS, CEISAM UMR 6230, F-44000 Nantes, France; Institut Universitaire de France, 75005 Paris, France; orcid.org/0000-0002-4217-0708; Email: Denis.Jacquemin@univ-nantes.fr

Authors

Pierre-François Loos – Laboratoire de Chimie et Physique Quantiques, Université de Toulouse, CNRS, UPS, 31400 Toulouse, France; orcid.org/0000-0003-0598-7425

Filippo Lipparini – Dipartimento di Chimica e Chimica Industriale, University of Pisa, S6124 Pisa, Italy; orcid.org/0000-0002-4947-3912

Complete contact information is available at: <https://pubs.acs.org/doi/10.1021/acs.jpcllett.3c03042>

Notes

The authors declare no competing financial interest.

■ ACKNOWLEDGMENTS

The authors thank P. de Silva, S. Odoh, Y. Olivier, and J. C. Sancho-Garcia for their helpful comments on this work. The authors are thankful for the generous allocations of time by the CCIPL/GliCID computational center installed in Nantes. P.-F.L. thanks the European Research Council (ERC) under the European Union's Horizon 2020 research and innovation programme (Grant Agreement No. 863481) for funding.

■ REFERENCES

- (1) Ehrmaier, J.; Rabe, E. J.; Pristash, S. R.; Corp, K. L.; Schlenker, C. W.; Sobolewski, A. L.; Domcke, W. Singlet–Triplet Inversion in Heptazine and in Polymeric Carbon Nitrides. *J. Phys. Chem. A* **2019**, *123*, 8099–8108.
- (2) de Silva, P. Inverted Singlet–Triplet Gaps and Their Relevance to Thermally Activated Delayed Fluorescence. *J. Phys. Chem. Lett.* **2019**, *10*, 5674–5679.
- (3) Ricci, G.; San-Fabián, E.; Olivier, Y.; Sancho-García, J. C. Singlet–Triplet Excited-State Inversion in Heptazine and Related Molecules: Assessment of TD-DFT and ab initio Methods. *ChemPhysChem* **2021**, *22*, 553–560.
- (4) Pollice, R.; Friederich, P.; Lavigne, C.; Gomes, G. d. P.; Aspuru-Guzik, A. Organic Molecules with Inverted Gaps Between First Excited Singlet and Triplet States and Appreciable Fluorescence Rates. *Matter* **2021**, *4*, 1654–1682.
- (5) Dinkelbach, F.; Bracker, M.; Kleinschmidt, M.; Marian, C. M. Large Inverted Singlet–Triplet Energy Gaps Are Not Always Favorable for Triplet Harvesting: Vibronic Coupling Drives the (Reverse) Intersystem Crossing in Heptazine Derivatives. *J. Phys. Chem. A* **2021**, *125*, 10044–10051.
- (6) Ghosh, S.; Bhattacharyya, K. Origin of the Failure of Density Functional Theories in Predicting Inverted Singlet–Triplet Gaps. *J. Phys. Chem. A* **2022**, *126*, 1378–1385.
- (7) Aizawa, N.; Pu, Y.-J.; Harabuchi, Y.; Nihonyanagi, A.; Ibuka, R.; Inuzuka, H.; Dhara, B.; Koyama, Y.; Nakayama, K.-i.; Maeda, S.; et al. Delayed Fluorescence from Inverted Singlet and Triplet Excited States. *Nature* **2022**, *609*, 502–506.
- (8) Ricci, G.; Sancho-García, J.-C.; Olivier, Y. Establishing Design Strategies for Emissive Materials With an Inverted Singlet–Triplet Energy Gap (INVEST): a Computational Perspective on how Symmetry Rules the Interplay Between Triplet Harvesting and Light Emission. *J. Mater. Chem. C* **2022**, *10*, 12680–12698.
- (9) Tučková, L.; Straka, M.; Valiev, R. R.; Sundholm, D. On the Origin of the Inverted Singlet–Triplet Gap of the 5th Generation Light-Emitting Molecules. *Phys. Chem. Chem. Phys.* **2022**, *24*, 18713–18721.
- (10) Monino, E.; Loos, P.-F. Connections and Performances of Green's Function Methods for Charged and Neutral Excitations. *J. Chem. Phys.* **2023**, *159*, 034105.
- (11) Drwal, D.; Matousek, M.; Golub, P.; Tucholska, A.; Hapka, M.; Brabec, J.; Veis, L.; Pernal, K. The Role of Spin Polarization and Dynamic Correlation in Singlet–Triplet Gap Inversion of Heptazine Derivatives. *J. Chem. Theory Comput.* **2023**, *19*, 7606–7616.
- (12) Terence Blaskovits, J.; Garner, M. H.; Corminboeuf, C. Symmetry-Induced Singlet–Triplet Inversions in Non-Alternant Hydrocarbons. *Angew. Chem., Int. Ed.* **2023**, *62*, No. e202218156.
- (13) Dreuw, A.; Hoffmann, M. The Inverted Singlet–Triplet Gap: a Vanishing Myth? *Front. Chem.* **2023**, *11*, 1239604.
- (14) Sandoval-Salinas, M. E.; Ricci, G.; Pérez-Jiménez, A. J.; Casanova, D.; Olivier, Y.; Sancho-García, J. C. Correlation vs. Exchange Competition Drives the Singlet–Triplet Excited-State Inversion in Non-Alternant Hydrocarbons. *Phys. Chem. Chem. Phys.* **2023**, *25*, 26417–26428.
- (15) Sanz-Rodrigo, J.; Ricci, G.; Olivier, Y.; Sancho-García, J. C. Negative Singlet–Triplet Excitation Energy Gap in Triangle-Shaped Molecular Emitters for Efficient Triplet Harvesting. *J. Phys. Chem. A* **2021**, *125*, 513–522.
- (16) Sobolewski, A. L.; Domcke, W. Excited-State Singlet–Triplet Inversion in Hexagonal Aromatic and Heteroaromatic Compounds. *Phys. Chem. Chem. Phys.* **2023**, *25*, 21875–21882.
- (17) Actis, A.; Melchionna, M.; Filippini, G.; Fornasiero, P.; Prato, M.; Chiesa, M.; Salvadori, E. Singlet–Triplet Energy Inversion in Carbon Nitride Photocatalysts. *Angew. Chem., Int. Ed.* **2023**, *62*, No. e202313540.
- (18) Loos, P.-F.; Jacquemin, D. A Mountaineering Strategy to Excited States: Highly Accurate Energies and Benchmarks for Bicyclic Systems. *J. Phys. Chem. A* **2021**, *125*, 10174–10188.
- (19) Lee, T. J.; Taylor, P. R. A Diagnostic for Determining the Quality of Single-Reference Electron Correlation Methods. *Int. J. Quantum Chem.* **1989**, *36*, 199–207.
- (20) Véral, M.; Scemama, A.; Caffarel, M.; Lipparini, F.; Boggio-Pasqua, M.; Jacquemin, D.; Loos, P.-F. QUESTDB: a Database of Highly-Accurate Excitation Energies for the Electronic Structure Community. *WIREs Comput. Mol. Sci.* **2021**, *11*, No. e1517.
- (21) Leupin, W.; Wirz, J. Low-Lying Electronically Excited States of Cycl[3.3.3]azine, a Bridged 12 π -Perimeter. *J. Am. Chem. Soc.* **1980**, *102*, 6068–6075.
- (22) Loos, P.-F.; Jacquemin, D. Evaluating 0–0 Energies with Theoretical Tools: a Short Review. *ChemPhotoChem.* **2019**, *3*, 684–696.
- (23) Loos, P.-F.; Jacquemin, D. Chemically Accurate 0–0 Energies with not-so-Accurate Excited State Geometries. *J. Chem. Theory Comput.* **2019**, *15*, 2481–2491.
- (24) Goerigk, L.; Moellmann, J.; Grimme, S. Computation of Accurate Excitation Energies for Large Organic Molecules with Double-Hybrid Density Functionals. *Phys. Chem. Chem. Phys.* **2009**, *11*, 4611–4620.
- (25) Jacquemin, D.; Planchat, A.; Adamo, C.; Mennucci, B. A TD-DFT Assessment of Functionals for Optical 0–0 Transitions in Solvated Dyes. *J. Chem. Theory Comput.* **2012**, *8*, 2359–2372.
- (26) Winter, N. O. C.; Graf, N. K.; Leutwyler, S.; Hättig, C. Benchmarks for 0–0 Transitions of Aromatic Organic Molecules:

DFT/B3LYP, ADC(2), CC2, SOS-CC2 and SCS-CC2 Compared to High-resolution Gas-Phase Data. *Phys. Chem. Chem. Phys.* **2013**, *15*, 6623–6630.

(27) Sobolewski, A. L.; Domcke, W. Are Heptazine-Based Organic Light-Emitting Diode Chromophores Thermally Activated Delayed Fluorescence or Inverted Singlet–Triplet Systems? *J. Phys. Chem. Lett.* **2021**, *12*, 6852–6860.

(28) Pios, S.; Huang, X.; Sobolewski, A. L.; Domcke, W. Triangular Boron Carbon Nitrides: An Unexplored Family of Chromophores with unique Properties for Photocatalysis and Optoelectronics. *Phys. Chem. Chem. Phys.* **2021**, *23*, 12968–12975.

(29) Sancho-García, J. C.; Brémond, E.; Ricci, G.; Pérez-Jiménez, A. J.; Olivier, Y.; Adamo, C. Violation of Hund's rule in molecules: Predicting the excited-state energy inversion by TD-DFT with double-hybrid methods. *J. Chem. Phys.* **2022**, *156*, 034105.

(30) Alipour, M.; Izadkhast, T. Do any Types of Double-Hybrid Models Render the Correct Order Of Excited State Energies in Inverted Singlet–Triplet Emitters? *J. Chem. Phys.* **2022**, *156*, 064302.

(31) Curtis, K.; Adeyiga, O.; Suleiman, O.; Odoh, S. O. Building on the Strengths of a Double-Hybrid Density Functional for Excitation Energies and Inverted Singlet–Triplet Energy Gaps. *J. Chem. Phys.* **2023**, *158*, 024116.

(32) Frisch, M. J.; Trucks, G. W.; Schlegel, H. B.; Scuseria, G. E.; Robb, M. A.; Cheeseman, J. R.; Scalmani, G.; Barone, V.; Petersson, G. A.; Nakatsuji, H.; et al. *Gaussian 16 Revision A.03*. 2016; Gaussian Inc. Wallingford CT.

(33) Stanton, J. F.; Gauss, J.; Cheng, L.; Harding, M. E.; Matthews, D. A.; Szalay, P. G. In *CFOUR, Coupled-Cluster Techniques for Computational Chemistry, a Quantum-Chemical Program Package* with contributions from A. A. Auer, R. J. Bartlett, U. Benedikt, C. Berger, D. E. Bernholdt, Y. J. Bomble, O. Christiansen, F. Engel, R. Faber, M. Heckert, O. Heun, M. Hilgenberg, C. Huber, T.-C. Jagau, D. Jonsson, J. Jusélius, T. Kirsch, K. Klein, W. J. Lauderdale, F. Lipparini, T. Metzroth, L. A. Mück, D. P. O'Neill, D. R. Price, E. Prochnow, C. Puzzarini, K. Ruud, F. Schiffmann, W. Schwalbach, C. Simmons, S. Stopkowitz, A. Tajti, J. Vázquez, F. Wang, and J. D. Watts and the integral packages MOLECULE (J. Almlöf and P. R. Taylor), PROPS (P.R. Taylor), ABACUS (T. Helgaker, H. J. Aa. Jensen, P. Jørgensen, and J. Olsen), and ECP routines by A. V. Mitin and C. van Wüllen, 2010; for the current version, see <http://www.cfour.de>.

(34) Matthews, D. A.; Cheng, L.; Harding, M. E.; Lipparini, F.; Stopkowitz, S.; Jagau, T.-C.; Szalay, P. G.; Gauss, J.; Stanton, J. F. Coupled-Cluster Techniques for Computational Chemistry: The CFOUR Program Package. *J. Chem. Phys.* **2020**, *152*, 214108.

(35) Loos, P.-F.; Lipparini, F.; Matthews, D. A.; Blondel, A.; Jacquemin, D. A Mountaineering Strategy to Excited States: Revising Reference Values with EOM-CC4. *J. Chem. Theory Comput.* **2022**, *18*, 4418–4427.

(36) Aidas, K.; Angeli, C.; Bak, K. L.; Bakken, V.; Bast, R.; Boman, L.; Christiansen, O.; Cimiraglia, R.; Coriani, S.; Dahle, P.; et al. The Dalton Quantum Chemistry Program System. *WIREs Comput. Mol. Sci.* **2014**, *4*, 269–284.

(37) Christiansen, O.; Koch, H.; Jørgensen, P. Response Functions in the CC3 Iterative Triple Excitation Model. *J. Chem. Phys.* **1995**, *103*, 7429–7441.

(38) Kowalski, K.; Piecuch, P. The Active-Space Equation-of-Motion Coupled-Cluster Methods for Excited Electronic States: Full EOMCCSDt. *J. Chem. Phys.* **2001**, *115*, 643–651.

(39) Matthews, D. A.; Stanton, J. F. A new Approach to Approximate Equation-Of-Motion Coupled Cluster with Triple Excitations. *J. Chem. Phys.* **2016**, *145*, 124102.

(40) Nottoli, T.; Gauss, J.; Lipparini, F. A Black-Box, General Purpose Quadratic Self-Consistent Field Code with and without Cholesky Decomposition of the Two-Electron Integrals. *Mol. Phys.* **2021**, *119*, No. e1974590.

(41) Head-Gordon, M.; Rico, R. J.; Oumi, M.; Lee, T. J. A Doubles Correction to Electronic Excited States From Configuration

Interaction in the Space of Single Substitutions. *Chem. Phys. Lett.* **1994**, *219*, 21–29.

(42) Dreuw, A.; Wormit, M. The Algebraic Diagrammatic Construction Scheme for the Polarization Propagator for the Calculation of Excited States. *WIREs Comput. Mol. Sci.* **2015**, *5*, 82–95.

(43) Christiansen, O.; Koch, H.; Jørgensen, P. The Second-Order Approximate Coupled Cluster Singles and Doubles Model CC2. *Chem. Phys. Lett.* **1995**, *243*, 409–418.

(44) Balasubramani, S. G.; Chen, G. P.; Coriani, S.; Diedenhofen, M.; Frank, M. S.; Franzke, Y. J.; Furche, F.; Grotjahn, R.; Harding, M. E.; Hättig, C.; et al. TURBOMOLE: Modular Program Suite for ab initio Quantum-Chemical and Condensed-Matter Simulations. *J. Chem. Phys.* **2020**, *152*, 184107.

(45) TURBOMOLE V7.3 2018, a development of University of Karlsruhe and Forschungszentrum Karlsruhe GmbH, 1989–2007, TURBOMOLE GmbH, since 2007.

(46) Hättig, C.; Weigend, F. CC2 Excitation Energy Calculations on Large Molecules Using the Resolution of the Identity Approximation. *J. Chem. Phys.* **2000**, *113*, 5154–5161.

(47) Neese, F.; Wennmohs, F.; Becker, U.; Riplinger, C. The ORCA Quantum Chemistry Program Package. *J. Chem. Phys.* **2020**, *152*, 224108.

(48) Chai, J.-D.; Mao, S.-P. Seeking for Reliable Double-Hybrid Density Functionals Without Fitting Parameters: The PBE0-2 Functional. *Chem. Phys. Lett.* **2012**, *538*, 121–125.

(49) Casanova-Páez, M.; Goerigk, L. Time-Dependent Long-Range-Corrected Double-Hybrid Density Functionals with Spin-Component and Spin-Opposite Scaling: A Comprehensive Analysis of Singlet–Singlet and Singlet–Triplet Excitation Energies. *J. Chem. Theory Comput.* **2021**, *17*, 5165–5186.